Development 128, 5005-5015 (2001)
Printed in Great Britain © The Company of Biologists Limited 2001
DEV3527

Drosophila Amphiphysin is implicated in protein localization and membrane morphogenesis but not in synaptic vesicle endocytosis

Andrew C. Zelhof[1,3,*], Hong Bao[2], Robert W. Hardy[3], Azam Razzaq[4,5], Bing Zhang[2] and Chris Q. Doe[1,*]

[1]Institute of Neuroscience, HHMI, University of Oregon 1254, Eugene, OR 97403, USA
[2]Section of Neurobiology, Institute for Cellular and Molecular Biology, University of Texas at Austin. Austin, TX 78712, USA
[3]Department of Biology, HHMI, University of California, San Diego. La Jolla, CA 92093, USA
[4]Department of Genetics, University of Cambridge, Downing Street, Cambridge CB2 3EH, UK
[5]Department of Biochemistry, University of Cambridge, Tennis Court Road, Cambridge CB2 1QW, UK
*Authors for correspondence (e-mail: cdoe@uoneuro.uoregon.edu and azelhof@biomail.ucsd.edu)

Accepted 26 September 2001

SUMMARY

Amphiphysin family members are implicated in synaptic vesicle endocytosis, actin localization and one isoform is an autoantigen in neurological autoimmune disorder; however, there has been no genetic analysis of Amphiphysin function in higher eukaryotes. We show that *Drosophila* Amphiphysin is localized to actin-rich membrane domains in many cell types, including apical epithelial membranes, the intricately folded apical rhabdomere membranes of photoreceptor neurons and the postsynaptic density of glutamatergic neuromuscular junctions. Flies that lack all Amphiphysin function are viable, lack any observable endocytic defects, but have abnormal localization of the postsynaptic proteins Discs large, Lethal giant larvae and Scribble, altered synaptic physiology, and behavioral defects. Misexpression of Amphiphysin outside its normal membrane domain in photoreceptor neurons results in striking morphological defects. The strong misexpression phenotype coupled with the mild mutant and lack of phenotypes suggests that Amphiphysin acts redundantly with other proteins to organize specialized membrane domains within a diverse array of cell types.

Key words: Synapse, Postsynaptic density, Apical membrane, Membrane morphogenesis, *Drosophila*

INTRODUCTION

The creation of specialized membrane regions is important for establishing cell polarity and for the proper function of many differentiated cell types. Genetic and biochemical experiments have identified numerous proteins involved in the formation of distinct membrane domains; in neurons and yeast, one of these proteins is Amphiphysin (Amph; Amp – FlyBase). Vertebrate Amph I protein was discovered because of its enrichment in brain presynaptic terminal membrane preparations (Lichte et al., 1992), whereas Amph II is more widely expressed (Butler et al., 1997; Ramjaun et al., 1997). Both Amph I and II have an N-terminal coiled-coil domain, a central proline-rich domain and a C-terminal SH3 domain. Mutant analysis of vertebrate Amph I and II has not been described, but most evidence suggests that Amph proteins are involved in endocytosis, particularly in synaptic vesicle recycling (Wigge and McMahon, 1998). Amph I is concentrated at presynaptic terminals, and expression of the SH3 domain of Amph I can block endocytosis in neurons or fibroblasts, leading to concomitant accumulation of clathrin coated pits at the plasma membrane (Shupliakov et al., 1997; Wigge et al., 1997). In addition, the Amph I central region binds the endocytic proteins α-Adaptin and Clathrin, while the SH3 domain interacts with the endocytic proteins Dynamin and Synaptojanin (David et al., 1996; Grabs et al., 1997; McPherson et al., 1996).

The role of Amphiphysin family members may not be limited to endocytosis. Vertebrate Amph II does localize to presynaptic sites, however, Amph II isoforms lacking the α-Adaptin-binding central domain are expressed in skeletal muscle (Butler et al., 1997). How, or if, these isoforms modulate endocytosis is not known. A *S. cerevisiae* Amph homolog, *rvs167*, shows conservation of the coiled-coil and SH3 domains, but the central domain is not well conserved nor is it needed for function (Sivadon et al., 1997). *rvs167* protein localizes to actin-rich cortical patches during G_1 phase, and then relocates to the bud site or the leading edge during schmoo formation (Balguerie et al., 1999). Yeast that lack *rvs167* and the related *rvs161* gene are viable but show abnormal cell shape, disorganization of the actin cytoskeleton during bud emergence and mating, and random bud site selection in diploid cells (Bauer et al., 1993; Sivadon et al., 1995).

We present the in vivo characterization of the single *Drosophila amph* (*Amp* – FlyBase) gene. We show that Amph protein is localized postsynaptically at neuromuscular junctions and is required for the localization of several postsynaptic proteins but not synaptic vesicle recycling. We also show that Amph is localized to specialized membrane domains in both epithelial and neural cell types, where it is

implicated in recruiting or stabilizing cortical proteins and organizing changes in membrane morphology.

MATERIALS AND METHODS

DNA constructs

The expressed sequence tags (ESTs) LD19810, LD02678, LD16210, HL01753, representing cDNAs of Amphiphysin were obtained from Berkeley *Drosophila* Genome Project (via Research Genetics). Each EST was sequenced. The RT-ISOC cDNA was identified and isolated via a reverse transcriptase and first strand synthesis (SuperScript II – Stratagene) with the following primer: 5′-GGACCACA-GAGGAATTACAT-3′. The nested primer pair (5′-CCACAG-AGCAAGTGTTCCACA-3′/5′-CCCCAGTTTGTCGCTTCAGAT-3′) was subsequently used for amplification. The PCR products were cloned into the pCRII-TOPO vector (Invitrogen) and three independent clones for each were sequenced for conformation of alternative splicing. The *Sal*I/*Spe*I fragment representing the

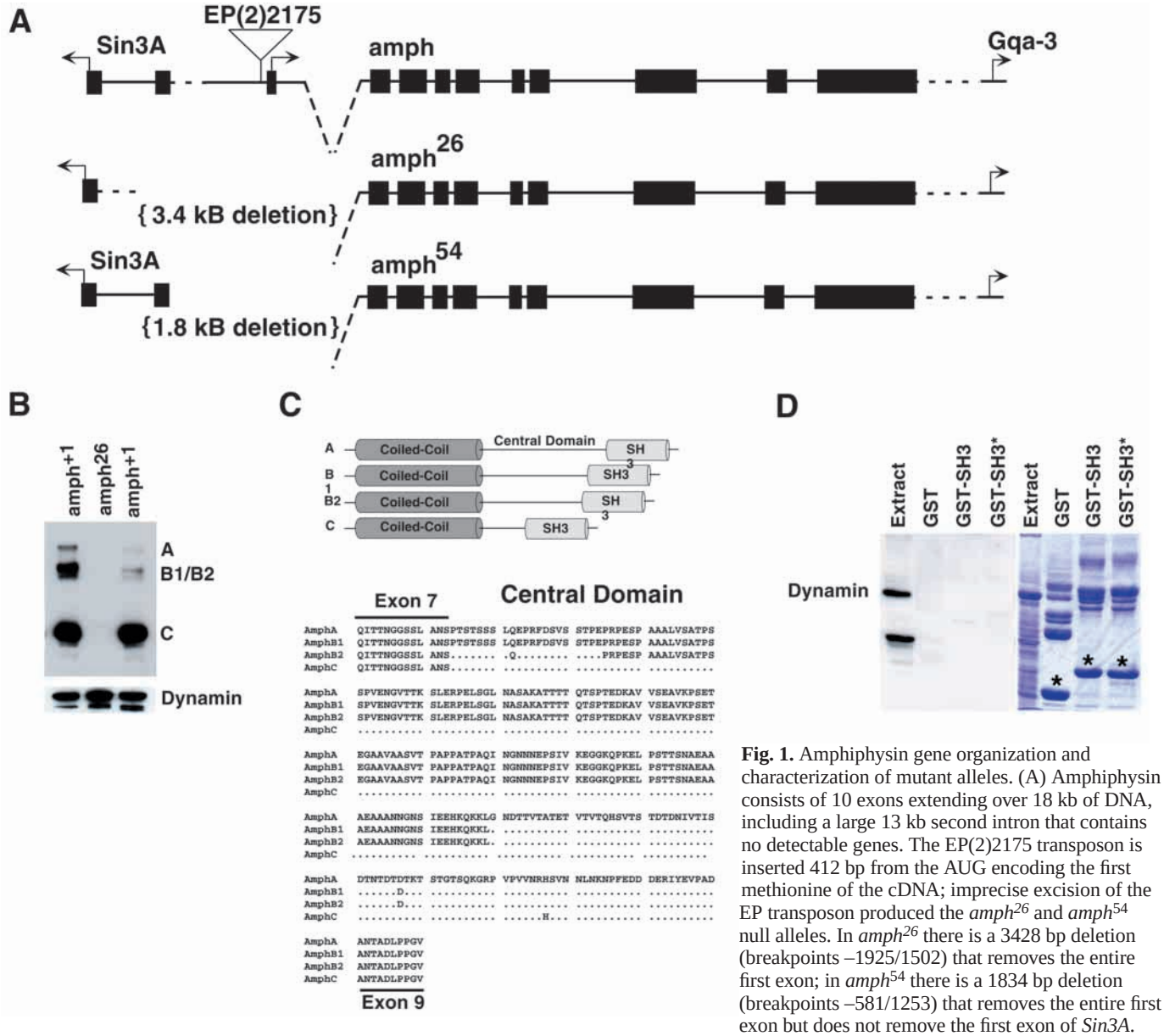

Fig. 1. Amphiphysin gene organization and characterization of mutant alleles. (A) Amphiphysin consists of 10 exons extending over 18 kb of DNA, including a large 13 kb second intron that contains no detectable genes. The EP(2)2175 transposon is inserted 412 bp from the AUG encoding the first methionine of the cDNA; imprecise excision of the EP transposon produced the *amph*^{26} and *amph*^{54} null alleles. In *amph*^{26} there is a 3428 bp deletion (breakpoints –1925/1502) that removes the entire first exon; in *amph*^{54} there is a 1834 bp deletion (breakpoints –581/1253) that removes the entire first exon but does not remove the first exon of *Sin3A*. All phenotypes are observed with either mutant. The *Sin3A* and *Gqα-3* genes are adjacent to the *amph* gene, but neither *amph* mutation affects the coding sequences of *Sin3A* or *Gqα-3* genes, and the *Sin3A* and *amph*^{26} mutations complement each other (A. Razzaq, personal communication), consistent with *amph*^{26} having no effect on Sin3A function. (B) Western analysis of *Drosophila* extracts from Amphiphysin mutant and precise excisions (*amph*$^{+1}$). In each of the putative null mutants, *amph*^{26} and *amph*^{54} (data not shown), there is no immunoreactivity detected. (C) Schematic representations of the four Amph isoforms. In each case, the alternative splicing occurs in exon 8, reducing or eliminating the central domain of Amphiphysin (top); sequence analysis of the four isoforms from the end of exon 7 to the start of exon 9 (bottom). (D) *Drosophila* Amphiphysin does not interact with *Drosophila* Dynamin: western analysis and Coomassie staining of Dynamin binding to the SH3 domain of Amphiphysin. *Drosophila* extract was mixed with three different fusion proteins: GST, GST fused to the SH3 domain of Amph (GST-SH3) and GST fused to a mutated form of the SH3 domain (GST-SH3*). In each case, we could not detect any binding of Dynamin to the GST proteins. The asterisks indicate the GST proteins.

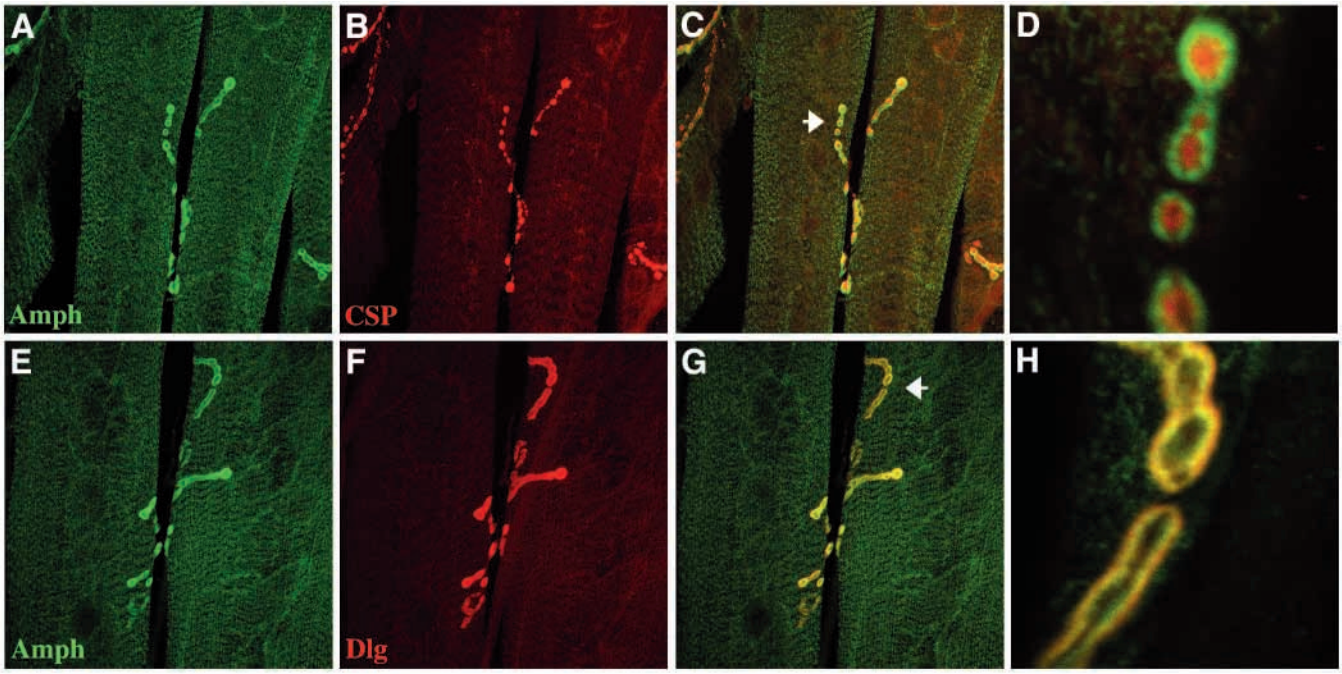

Fig. 2. Amphiphysin is postsynaptic at the larval neuromuscular junction. (A-D) Amphiphysin (green) does not colocalize with presynaptic marker Cysteine String Protein (red) at third instar neuromuscular synapses; Amph staining surrounds the CSP staining, as expected for a postsynaptic protein. Low-magnification view of the NMJs at muscle 6 and 7 of abdominal segment 2 showing Amph (A), Csp (B) and the merged image (C); a high-magnification image of the region indicated with an arrow in C is shown in D. (E-H) Amphiphysin (green) is precisely colocalized with the postsynaptic marker Discs large (red) at third instar type I neuromuscular synapses. Low-magnification view showing Amph (E), Dlg (F) and the merged image (G); a high-magnification image of the region indicated with an arrow in G is shown in H.

alternative spliced region of isoform C as well as the 3′ end of Amphiphysin was substituted into the LD02678 EST via a *Sal*I/*Nhe*I digest to create RT-ISOC, a full-length cDNA. UAS constructs: *Eco*RI/*Xho*I fragments of LD19810 (AmphA) and HL01753 (Amph B2) were cloned into PUAST (Brand and Perrimon, 1993) and transformed into flies.

Genomic analysis of *amph*^{26} and *amph*^{54}

Genomic DNA was isolated from homozygous animals and subjected to a series of PCR reactions. The PCR reactions were designed to assay the entire genomic interval of *amph* for deleted segments. The following lists denotes the 5′ position of the primer pairs used relative to alanine (+1) of the first methionine of the cDNA: –2846/2044; 1077/2372; 4669/6095; 10,213/11,586; 12,799/13,483; 13,318/14,285; 13,734/15,410; 15,078/15982; 15,570/17,055; 16,633/17,764. Only the primer pair of 1077/2372 did not result in a band for either *amph*^{26} or *amph*^{54}, but a subsequent PCR reaction using outside primers –2846/2372 did result in two PCR products ~1.6 kb and 3.4 kb (expected size 5.2 kb) for each of the above mutants, respectively. The PCR products were cloned and sequenced to identify the precise breakpoints of the deleted segment.

GST fusion proteins

The following regions of Amphiphysin were cloned into pGEX-4T1 (Pharmacia): amino acids 8-361, representing the coil-coiled domain, and 523-602, representing the SH3 domain. A third GST fusion protein was created that contained the SH3 domain but had these changes: G592R, P595L and A596G. The *Eco*RI/*Xho*I fragments of ESTs LD19810 and HL01753 were cloned into pGEX-4T1.

Immunohistochemistry and electron microscopy

Rabbit polyclonal antibodies to Amph were generated against the N-terminal (9907) and the SH3 (9906) GST fusion proteins. Embryos and larvae were stained as previously described (McDonald and Doe, 1997). Adult *Drosophila* heads were frozen in OCT and 14 μm sections were cut and fixed for 10 minutes in PEMFA (McDonald and Doe, 1997). The tissue was blocked in PBTB (phosphate-buffered saline (PBS) and 0.1% Triton X with 1% bovine serum albumin (BSA)) for 30 minutes, incubated in primary antibody (in PBTB) overnight at 4°C, washed in PBTB, incubated in secondary antibody for 2 hours at room temperature, washed in PBT (PBS and 0.1% Triton X), and mounted as previously described (Zelhof et al., 1997). The following primary antibodies were used: rabbit anti-Amph (9906 and 9907; 1:100), guinea pig anti-Dlg (1:1000), mouse anti-CSP (ab49; 1:50), mouse anti-Myc (Calbiochem; 1:100), sheep anti-Bifocal (1:1000), rabbit anti-Scribble (1:100), rabbit anti-LglC (1:100), mouse mAb2A12 (1:5), rhodamine-conjugated phalloidin (1:100-1000; Molecular Probes) and goat FITC-conjugated anti-horseradish peroxidase (HRP) (1:100). Histochemical detection was performed using the Vectastain Elite Kit (Vector Labs) in conjunction with metal enhanced DAB substrate (Pierce). Species-specific FITC-, Texas Red- and Cy5-conjugated secondary antibodies were obtained from Jackson Immunoresearch Labs (1:200). Electron microscopy of adult *Drosophila* eyes was as previously described (Baker et al., 1994).

Drosophila protein extracts and western analysis

Tissue was placed in extraction/binding buffer (EB; 100 mM KCl, 20 mM Hepes, 5% Glycerol, 10 mM EDTA, 0.1% Triton X with the proteinase inhibitors Aprotinin 1 μg/ml, Leupeptin 1 μg/ml, and Pepstatin 1 μg/ml), homogenized and sonicated. The mixture was spun and the supernatant was collected and an equal volume of 2× sample/loading buffer was added. All extracts were resolved by SDS-PAGE and then transferred to Immobilon-P (Millipore). Protein detection was as previously described (Baker et al., 1994). The anti-Amphiphysin serum (9906 or 9907) was used at 1:2500 and anti-Dynamin serum (shi-3) at 1:5000.

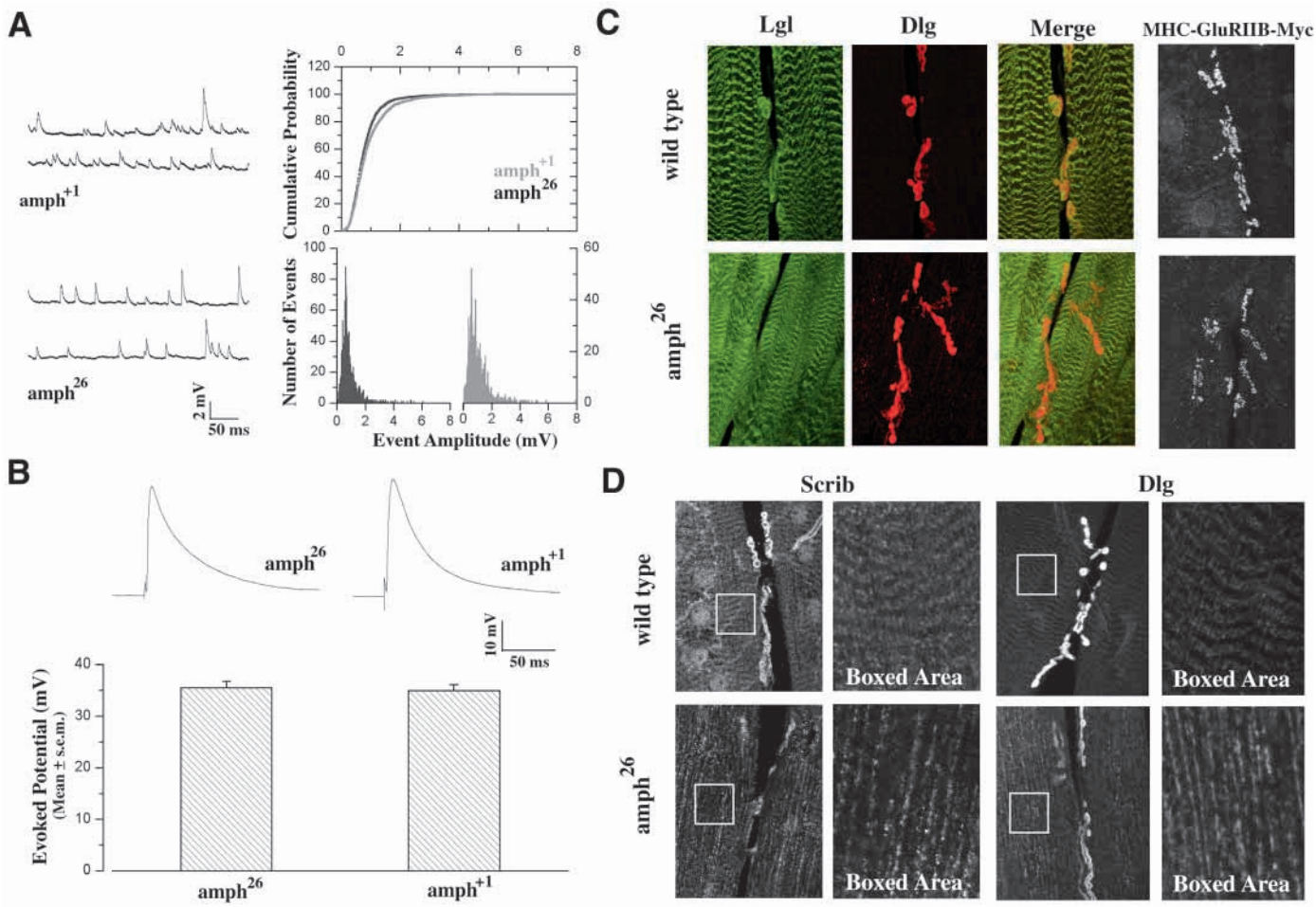

Fig. 3. Amphiphysin is required for postsynaptic protein localization and synaptic function at larval type I neuromuscular junctions. (A) Miniature excitatory junctional potentials (mEJP) recordings reveal there is a small but significant increase in quantal size in *amph* mutants. Left panels show representative traces of mEJPs from $amph^{26}$ mutant and wild-type ($amph^{+1}$) flies. Histograms and comparative cumulative plots are shown on the right. The average mEJP for the $amph^{+1}/amph^{+1}$ is 0.81±0.01 mV (n=2804) and for $amph^{26}/amph^{26}$ is 0.94±0.02 mV (n=2148) (P<0.05). (B) There is no change in the amplitude of the elicited response in *amph* mutants. Elicited response is measured as excitatory junctional potentials (EJPs) for $amph^{26}$ mutants and wild type ($amph^{+1}$). Representative EJP tracings from $amph^{26}/amph^{26}$ and $amph^{+1}/amph^{+1}$ larva (top). Histograms representing the average amplitude for each genotype (bottom): $amph^{26}/amph^{26}$ 35.5±1.29 mV (n=16) and $amph^{+1}/amph^{+1}$ 34.9±1.22 mV (n=15) P>0.1. (C) Immunohistochemical examination of the third instar NMJ of wild type (top) and $amph^{26}$ mutant (bottom) larva. The NMJs of muscles 6 and 7 of abdominal segment 2 are shown. The localization of Dlg, Lgl and GluRIIB are shown. In *amph* mutants, Lgl is absent from the synapse but still maintained in the M band of the muscle. GluRIIB protein localization at the NMJ is identical in wild type and $amph^{26}$ mutants. (D) Immunohistochemical examination of the third instar larval NMJ in wild type (top) and $amph^{26}$ mutants (bottom). The NMJs of muscle 6 and 7 of abdominal segment 2 are shown. The boxed areas represent the magnified views of the accompanying panels. In *amph* mutants, both Scrib and Dlg still show localization to the synapse but there is protein delocalized throughout the muscle.

Electrophysiology

Spontaneous miniature (minis or mEJP) and elicited synaptic potentials were recorded from bodywall muscles of third instar larvae in HL-3 solution using microelectrodes with an input resistance between 15 MΩ and 23 MΩ. Data were acquired and digitized using a PC computer with the use of pCLAMP 8 software (Axon Instruments). The analysis and presentation of figures were conducted on MiniAnalysis (Synaptosoft) and Origin (OriginLab). In all of the mini recordings, low extracellular Ca^{2+} (0.1 mM) and tetrodotoxin (TTX, 5 μM) were added to Ca^{2+}-free HL-3 solutions to minimize multiple quantal events (Zhang et al., 1998). Samples used for final analysis were obtained from at least five different larvae. Total number of events (n) were pooled together for quantal analysis in histograms, cumulative probability plots and statistics. To study elicited transmitter release, a suction electrode was used to stimulate motor nerve axons that innervate muscles 6, 7, 12 and 13 in HL-3 solutions containing 1 mM Ca^{2+}. At least three different larvae were used for data collection. All samples were recorded from muscles with resting potentials between –62 mV and –69 mV only. The resting potentials for $amph^{26}$ and $amph^{+1}$ were –63.9±0.88 mV and –64.4±0.49 mV, respectively. They were –65.4±-0.67 mV and –64.5±0.62 mV for $amph^{26}$; GluRIIB and control, respectively. There were no statistical differences between these resting potentials and the input resistances of the muscle cell. The amplitude of EJPs was analyzed for statistics using unpaired Student's t-test, while the comparison of quantal size was conducted using Kolmogorov-Smirnov test. All of the statistical data are presented as mean±s.e.m. P<0.05 is considered significant.

Fly stocks

amph mutant alleles ($amph^{26}$, $amph^{54}$ and $amph^{+1}$ (represents the

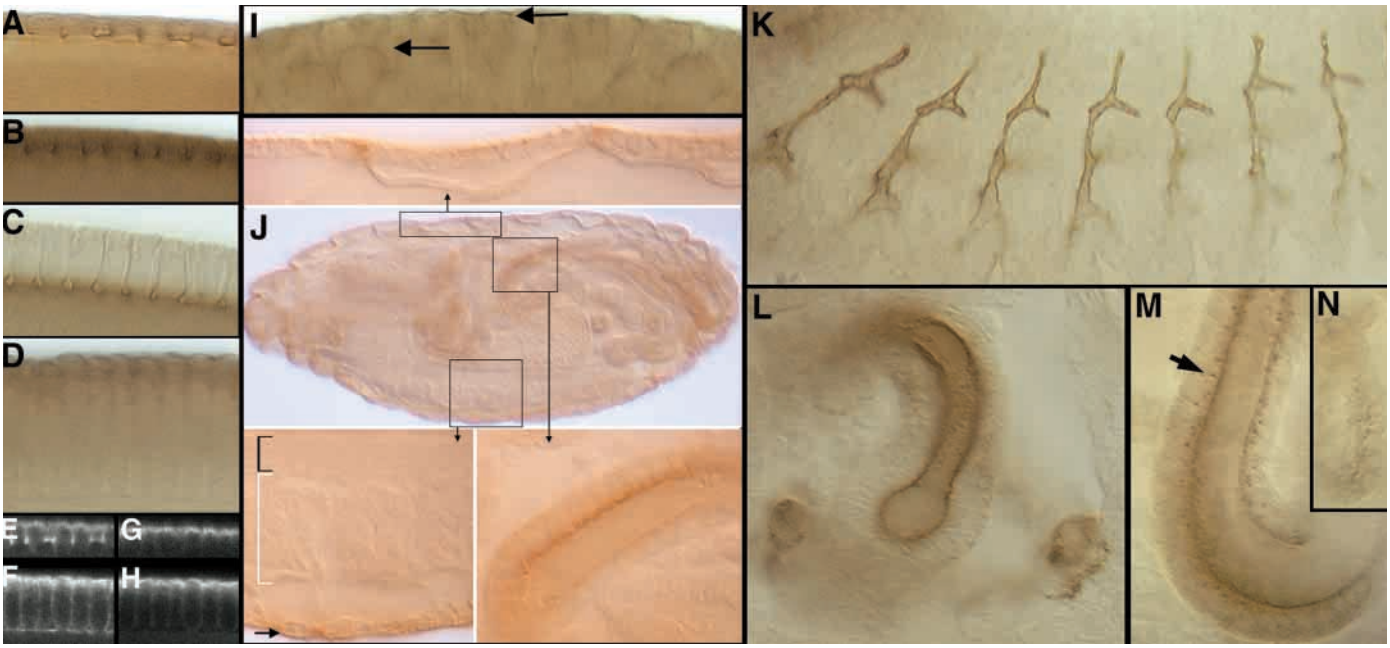

Fig. 4. Amphiphysin is localized to the apical membrane domain of epithelial and neural cell types. (A-D) Lateral views of a developmental time series of a stage 5 embryo stained for Amph. At early stage 5, the syncitial nuclei have migrated to the periphery and the membrane has begun to invaginate between the nuclei. Amph is first localized to the apical surface and migrates basally as the membrane extends inwards during cellularization. (D) Upon the completion of cellularization at the end of stage 5, Amph is again localized apically. (E-H) Double labels of Amph and Bifocal protein localization during early cellularization (E,G) and after completion of cellularization (F,H). Amph protein (E,F) is enriched at the invaginating membrane during cellularization, whereas Bifocal protein (G,H) remains localized to the apical membrane domain. (I) Amph is apical in ectoderm and neuroblasts. Lateral view of a stage 9 embryo showing apical Amph in the ventral ectoderm and in neuroblasts (arrows). (J) Lateral view of a stage 16 embryo to emphasize that Amph is not detected in the embryonic CNS (bottom left panel) when compared with the staining in the epidermis and trachea (top panel) and hindgut (bottom right panel). (K,L) Amph is detected at the apical (lumenal) membrane of tracheal tubules and of the esophagus. (K) Stage 15 embryo showing Amph expression at the apical surface in mature tracheal tubules. (L) Stage 15 embryo showing Amph expression in the esophagus. In addition, the non-epithelial secretory garland cells flanking the esophagus also express Amph. (M,N) Amph is localized to apical membrane and vesicles in internal tubular epithelia, such as the hindgut (M) and salivary glands (N). The arrow indicates Amph immunoreactive vesicles.

precise excision of the EP(2) 2175 P-element) were provided by Dr C. O'Kane. The *bifocal*^{R38} and *bifocal*^{R47} alleles were provided by Dr W. Chia. The transgenic flies MHC-GluRIIB-Myc and MHC-GluRIIA-Myc were provided by Dr C. Goodman. Df(2R)vg-C was obtained from the Bloomington Stock Center.

RESULTS

A single *amphiphysin* gene generates four protein isoforms

We identified *amph* in a misexpression screen (Rorth, 1996; Rorth et al., 1998) for genes that alter the branching pattern of sensory neuron axonal arbors. The transposon EP(2)2175 was inserted adjacent to the *amph* gene and produced a subtle disorganization of axon arborizations, which is due to the misexpression of *amph*. This *amph* gene is the only *amph* gene in *Drosophila* (Lloyd et al., 2000; Razzaq et al., 2000). We analyzed four *amph* ESTs and found that they represented three alternative splice isoforms encoding predicted proteins of 602 (AmphA), 522 (AmphB1) and 502 (AmphB2) amino acids that differ in the size of their central domain (Fig. 1). We generated antibodies to the Amph N- and C-terminal regions, and each antibody gave the predicted pattern on western blots, thus establishing the specificity of our antisera. In addition, both antisera detected a smaller 41 kDa band (AmphC) (Fig. 1B). We used RT-PCR from larval mRNA to confirm that all four proteins, including the 41 kDa AmphC isoform, are unique splice isoforms derived from the single *amph* gene. Each isoform contains the coiled-coil and SH3 domains (Fig. 1C).

Amph null mutants were created by imprecise excision of the EP(2)2175 transposon. Homozygous *amph*^{26} and *amph*^{54} flies were tested for protein expression using western blots and immunohistochemical staining of embryos, third instar neuromuscular junctions, and developing photoreceptor cells. We used antibodies that recognized the Amph N terminus, as well as antibodies recognizing the Amph C terminus, but we could not detect any protein expression (Fig. 1B). In addition, we mapped the lesions of *amph*^{26} and *amph*^{54}; both are deletions that remove the entire first exon and extend into the first intron (Fig. 1A). There is one predicted transcription start site in the 13 kb second intron (and no open reading frames), but we do not believe it is used because: (1) homozygous mutant embryos show no Amph protein; (2) using a primer representing the second putative start site, we could not detect any RT-PCR products (data not shown); and (3) all sequenced cDNAs contain the first exon and no alternative 5′ end was identified. As such, we conclude that both *amph*^{26} and *amph*^{54} are null alleles that produce no Amph protein product and do not affect the neighboring *Sin3A* gene.

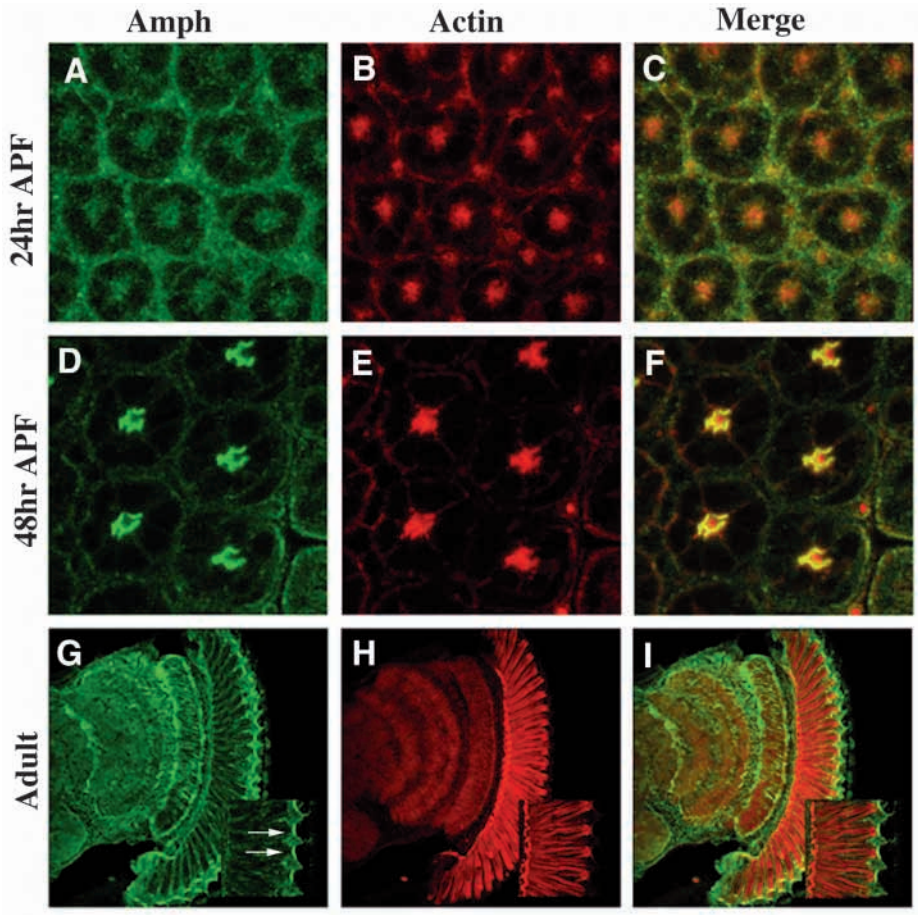

Fig. 5. Amphiphysin is localized to the apical membrane before rhabdomere formation in photoreceptor neurons. Amph protein (green) and F-actin (red) are shown in pupal photoreceptor neurons (A-F) or in adult eyes (G-I). Each image represents a single confocal section of a *z*-series. (A-C) Twenty-four hours APF, only actin accumulates at the apical surface of the photoreceptor cells, whereas Amph is found throughout the cell. (D-F) Forty-eight hours APF, Amph accumulates on the apical surface of the photoreceptor cells, where the rhabdomeres will develop. There is some overlap between F-actin and Amph, but F-actin becomes tightly colocalized with Amph only at 55 hours APF (see Fig. 7F). (G-I) In the adult eye, F-actin (red) strongly labels the rhabdomere membrane, whereas Amph (green) is specifically expressed in the lens-secreting cone cells above the rhabdomeres (arrows). Amph expression is also found in cells of the adult head.

amphiphysin mutants lack obvious endocytic defects in synaptic vesicle recycling

Given the wide tissue distribution of Amph (see Fig. 2, Fig. 4, Fig. 5), and the existence of only one *Drosophila amph* gene, we expected *amph* mutants to have severe pleiotropic defects and in particular endocytic defects. To our surprise, *amph* null mutant animals survive to adulthood, although larvae move sluggishly and adults do not fly.

We tried several approaches to detect an endocytic defect in *amph* mutants. In vertebrates, Amph is implicated in endocytosis via its interaction with Dynamin, but we can not detect an interaction between the SH3 domain of Amph and *Drosophila* Dynamin (Fig. 1D), nor do we see protein colocalization with Dynamin in the embryo, neuromuscular junction or at any location that shows Amph expression. In addition, we have not been able to detect genetic interactions between *amph* and the endocytic mutant *shibire* (encoding Dynamin), although other endocytic mutants such as *α-Adaptin* show sensitive genetic interactions with *shibire* (Gonzalez-Gaitan and Jackle, 1997). Last, we find that *amph* mutants have normal presynaptic physiological properties, eliminating a role for Amph in synaptic vesicle recycling (Fig. 3).

Amphiphysin protein is enriched at the postsynaptic density of larval neuromuscular junctions

In order to explain the locomoter defects of both larvae and adults, we examined the larval neuromuscular junction (NMJ). First, Amph localization can be detected in the muscle and shows enrichment at the NMJ (Fig. 2). To determine whether it is presynaptic or postsynaptic, we did colocalization experiments with a postsynaptic marker, Discs large (Dlg; Dlg1 – FlyBase) (Lahey et al., 1994), and a presynaptic protein marker, Cysteine String Protein (Csp) (Umbach et al., 1994; Zinsmaier et al., 1994). We find that Amph and the postsynaptic marker Dlg are perfectly colocalized (Fig. 2A-D), whereas Amph protein surrounds but does not colocalize with the presynaptic marker Csp (Fig. 2E-H). Thus, the majority of the Amph protein is postsynaptic, although we cannot exclude the possibility that there are low levels of Amph at the presynaptic side of the NMJ. In addition, Amph appears to be specifically localized to the type I Dlg^+ glutamatergic synapses but absent from type II and III synapses (data not shown), which are thought to contain other neurotransmitters and modulators (Anderson et al., 1988; Cantera and Nassel, 1992; Gorczyca et al., 1993; Monastirioti et al., 1995).

Amphiphysin is required for postsynaptic protein localization and function

Given that Amph is localized to the NMJ, we next assayed for structural and functional defects at the neuromuscular junction (NMJ). *amph* mutants show no defects in the localization of presynaptic marker proteins (e.g. Dynamin, Cysteine String Protein and HRP) and there are no defects in bouton structure or number. By contrast, several postsynaptic proteins showed abnormal localization in *amph* mutants. In wild-type larvae, type I glutamatergic synapses show postsynaptic enrichment of Dlg (Fig. 3C) (Lahey et al., 1994). In addition, two other proteins, Scribble (Scrib) and Lethal giant larvae (Lgl; L(2)gl – FlyBase), are colocalized with Dlg at the NMJ. Scrib, Lgl and Dlg are all tumor suppressor proteins that are colocalized in epithelia (Bilder et al., 2000). In *amph* mutants, there is a clear increase in Dlg and Scrib protein delocalized throughout

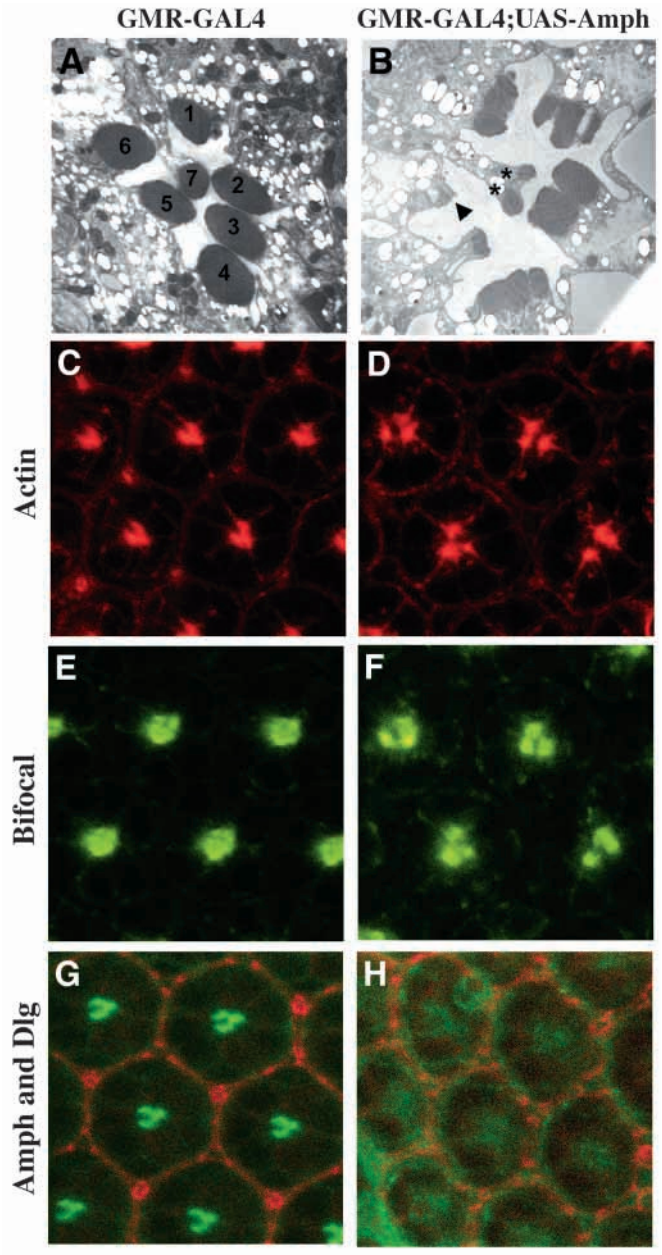

Fig. 6. Amphiphysin organizes the rhabdomere membrane domain in photoreceptor neurons. (A,B) Transmission electron microscopy analysis of photoreceptor cells overexpressing Amph. GMR-GAL4 is a transgenic line that contains the glass enhancer driving GAL4. This line provides strong expression of GAL4 in every cell posterior to the morphogenetic furrow. (A) GMR-GAL4 control. One copy of the transgenic line does not result in any detectable defects. (B) The addition of one copy of UAS-Amph results in split and ectopic rhabdomeres (asterisks) or the loss of rhabdomeres (arrowhead). (C,D) Optical sections through the developing retinal epithelium 55 hours APF stained for actin. (C) GMR-GAL4 control. F-Actin localizes in tight crescents on the apical surface of each photoreceptor cell. (D) GMR-GAL4 and UAS-Amph. The overexpression of Amph results in F-Actin accumulating in tight ball like structures versus the characteristic crescents seen in the control. (E,F) Optical sections through the developing retinal epithelium 55 hours APF stained for Bifocal. (E) GMR-GAL4 control. Bifocal localizes to the apical surface of photoreceptor cells. (F) GMR-GAL4 and UAS-Amph. Bifocal is mislocalized in each of the photoreceptor cells overexpressing Amph. (G,H) Optical sections through the developing retinal epithelium 55 hours APF stained for Discs large (red) and Amph (green). (G) GMR-GAL4 control. Amph shows normal apical localization. (H) GMR-GAL4 and UAS-Amph. The overexpression of Amph results in the delocalization of Amph from the apical surface of photoreceptor cells but overexpression does not affect patterning of the ommatidia.

the muscle (Fig. 3C) but we cannot detect a reduction at the synapse. *amph* mutants show a more severe Lgl phenotype: no Lgl protein can be detected at the synapse, although the localization of Lgl to the muscle M band is unaffected (Fig. 3C).

Dlg is considered to be a scaffold molecule for organizing the postsynaptic density, whereas the role of Lgl and Scrib at the synapse is not known. Changes in the localization of these proteins could potentially alter postsynaptic responsiveness to transmitter release. To test whether *amph* mutations alter synaptic physiology, we first measured the spontaneous release of transmitter by detecting the miniature excitatory junctional potentials (mEJPs). The amplitude of mEJPs (quantal size) is considered to be a measurement of the sensitivity of the muscle glutamate receptors to the spontaneous release of transmitter from single synaptic vesicles. We observed a small but statistically significant increase in mEJP amplitude in $amph^{26}$ mutants (0.94±0.02 mV; n=2148) compared with wild-type controls ($amph^{+1}$, 0.81±0.01 mV; n=2804, P<0.05, Kolmogorov-Smirnov test) (Fig. 3A). Although quantal size in *amph* mutants is increased, elicited transmitter release measured by the amplitude of EJPs was found to be similar between $amph^{26}$ mutant larvae and control larvae $amph^{+1}$: $amph^{26}$ was 35.5±1.29 mV (n=16) whereas $amph^{+1}$ was 34.9±1.22 mV (n=15) P>0.1 (Fig. 3B). The increase in quantal size suggests that the amount of transmitter per vesicle (i.e. quantum) is increased and/or that the postsynaptic receptors have become more sensitive to glutamate in the mutant. As Amph is primarily a postsynaptic protein, we reasoned that it is likely to play a direct role in regulation of the density or the ratio of glutamate receptor subtypes (DiAntonio et al., 1999). We tested this hypothesis by overexpressing GluRIIB levels in the muscle (see Materials and Methods) and examined whether it could rescue the mEJP phenotype. We found that increased GluRIIB levels lead to a decrease in the amplitude of mEJPs in both controls and *amph* mutants, but *amph* mutants still have a larger mEJP than controls ($amph^{26}$; GluRIIB is.56±0.005 mV, n=3308; $amph^{+1}$;GluRIIB is.42±0.005 mV, n=1734; P<0.05, Kolmogorov-Smirnov test). Consistent with these physiological data, we detected no significant change in the density of GlurRIIB receptors in *amph* mutants (Fig. 3C).

Amphiphysin localizes to apical membrane domains in epithelial and neural cell types

The localization and function of Amph at the postsynaptic density of Type I synapses, which are exclusively characterized by an elaborate subsynaptic reticulum (Atwood et al., 1993; Budnik et al., 1990; Jia et al., 1993), suggests that Amph may play a role in regulating membrane organization or in selective protein targeting. To further investigate this possibility, we performed a detailed examination of Amph localization and expression patterns in embryonic, larval, pupal and adult tissues. We detected Amph in diverse cell types and in all

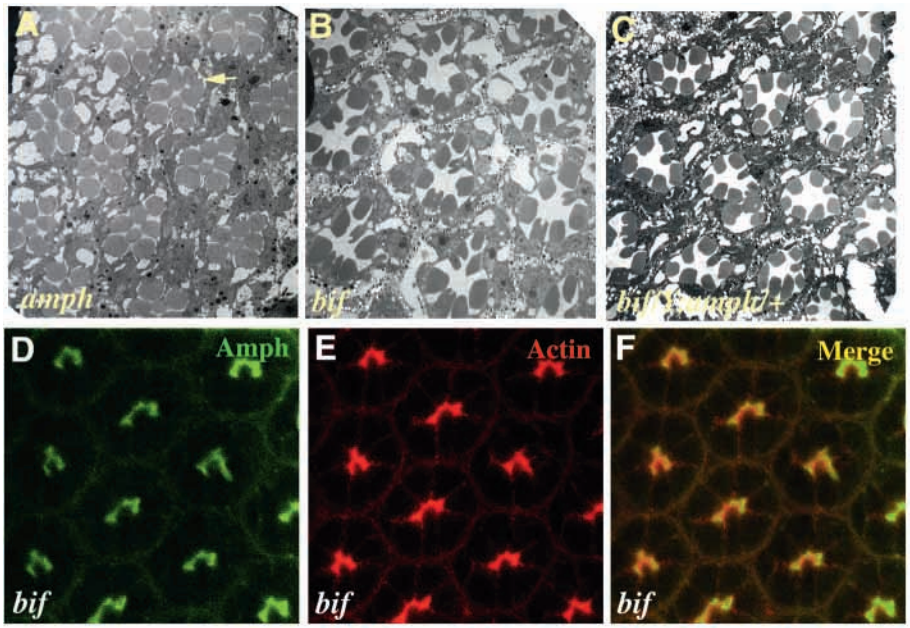

Fig. 7. Amph and Bifocal act oppositely for proper rhabdomere development. (A-C) Transmission electron micrographs of genetic combinations of Bifocal and Amph. (A) $amph^{26}/amph^{26}$ mutant. The rhabdomeres are closely packed and occasionally fused (arrow). (B) $bifocal^{R38}/bifocal^{R38}$. As reported previously, *bifocal* mutants have split and elongated rhabdomeres. (C) $bifocal^{R38}$/Y; $amph^{26}$/+. Removal of one copy of *amph* results in a partial rescue of the *bifocal* phenotype. First actin localization appears normal (data not shown) and subsequently fewer rhabdomeres are split and elongated. (D-F) Optical sections through the developing retinal epithelium 55 hours APF of a *bifocal* mutant stained for Amph (green) and F-actin (red) (D) Amph expression in $bifocal^{R38}/bifocal^{R38}$. Amph localization in a *bifocal* mutant still demarcates the apical surface but is very diffuse rather than a tight crescent. (E) F-Actin expression in $bifocal^{R38}/bifocal^{R38}$. Like Amph, Actin still localizes to the apical surface but shows diffuse staining. (F) F-Actin still colocalizes with Amph, as seen in normal development.

Amph-expressing cells, Amph is restricted both spatially and temporally to a specific domain of the plasma membrane, typically a domain that is undergoing membrane remodeling or where a submembrane protein scaffold is being assembled.

During embryogenesis, Amph is first detected during cellularization, as membrane is being inserted between each nuclei of the syncitial blastoderm stage embryo. Initially, Amph is detected at the apical surface of the precellular embryo (Fig. 4A). As the membrane extends inward (basally) during cellularization, Amph decorates the leading edge (Fig. 4B,C,E-F); this differs from Bifocal (Bahri et al., 1997), which consistently labels apical membrane domain (Fig. 4G-H). Upon completion of cellularization, Amph returns to the apical surface of the newly formed cells (Fig. 4D), where it is colocalized with many apical membrane markers (Fig. 4G,H). Amph is subsequently localized to the apical membrane domain in the ventral ectoderm and in the neuroblasts that delaminate from this ectoderm (Fig. 4I), as well to the apical membrane of tubular internal tissues such as the esophagus, hindgut, trachea and salivary glands (Fig. 4J-N). In many of these tissues, Amph is also robustly detected in small punctate presumptive vesicles within the cytoplasm of the cell (Fig. 4N); the identity of these vesicles is unknown. Amph expression is not detected in embryonic postmitotic neurons or muscles (Fig. 4J and data not shown), although it is detected in larval muscles. Surprisingly, our analysis of *amph* mutants and misexpression studies did not reveal any pronounced defects in process of cellularization, trachea formation or asymmetric localization of cell fate determinants during embryonic neuroblast divisions; further indication that Amph function is either not necessary or redundant with other proteins.

Amphiphysin aids in the organization of the rhabdomere membrane domain in photoreceptor neurons

Adult *Drosophila* photoreceptor cells are specialized neurons that have an apical microvillar stack of intricately folded membranes, the rhabdomere, that contains the light-sensing rhodopsin proteins. Twenty-four hours after puparium formation (APF) – before the formation of the apical microvilli – each photoreceptor shows F-actin accumulation at the apical membrane, while Amph is distributed more diffusely (Fig. 5A-C). Forty-eight hours APF, Amph has localized into a dense crescent at the apical cortex of each photoreceptor neuron as the first actin-filled apical microvilli can be detected (Fig. 5D-F). By 55 hours APF, F-actin and Amph are tightly colocalized at the apical membrane domain of each photoreceptor neuron (Fig. 7D-F and data not shown), and it is this domain that will subsequently give rise to the rhabdomere. In the adult, Amph is no longer expressed in the photoreceptor cells, but can be detected in the lens-secreting cone cells (Fig. 5G-I).

Given the accessibility of *Drosophila* photoreceptors to genetic, immunohistochemical and electron microscopic examination, we investigated whether Amph is required for the biogenesis of the rhabdomere as a model for its general role in membrane morphogenesis. Homozygous *amph* mutant adults have superficially normal eyes that respond to light correctly. However, electron microscopy of *amph* mutant eyes reveals that the rhabdomere membranes are unusually closely packed and occasionally fused, thus creating very little inter-rhabdomere space (Fig. 7A).

To further explore the role of Amph in the elaboration and formation of the rhabdomeres, we used GMR-GAL4 to overexpress Amph in the developing photoreceptor neurons. Overexpression of GMR-GAL4 alone or with a control UAS-GFP transgene had no effect on rhabdomere morphology (Fig. 6A). By contrast, overexpression of the Amph can produce outwardly normal eye but with a loss of all recognizable internal cell structure by electron microscopy (data not shown). More informative weaker phenotypes can be generated by expressing Amph at a lower temperature (where GAL4 is less active and there is less Amph protein as confirmed by western blots; data not shown). Overexpression of intermediate levels of Amph produce two to three smaller

rhabdomeres per cell, split rhabdomeres or no rhabdomeres (Fig. 6B). Despite the severe morphological defects, these photoreceptor neurons are functional, and overexpression of Amph does not affect photoreceptor neuron cell fate decisions.

The Amph overexpression eye phenotype (split/ectopic rhabdomeres) is similar to the loss-of-function *bifocal* mutant phenotype (Bahri et al., 1997) (Fig. 7B), suggesting that *amph* and *bifocal* may act in the same genetic pathway. Bifocal is a novel protein that is colocalized with Amph at the apical membrane of newly formed embryonic cells (Fig. 4E-G), as well as at the apical membrane of photoreceptor neurons. In photoreceptor neurons, Bifocal expression precedes Amph and lasts into adulthood (data not shown). *amph* mutants show normal Bifocal localization (data not shown), but *bifocal* mutants show delocalization of Amph into a broad apical domain matching that of F-actin, rather than its normal tight apical crescent (Fig. 7D,E). The *bifocal* mutant phenotype can be suppressed by reducing Amph gene dosage by 50% (Fig. 7C). Thus, bifocal-mediate localization of Amph to the future rhabdomere membrane domain is essential for normal eye development.

To determine the developmental origin of the *amph* overexpression phenotype, we assayed Amph, Bifocal and F-actin localization during rhabdomere development. Wild-type photoreceptors show an even distribution of Bifocal, Amph and F-actin at the apical surface of the cell (Fig. 6C,E). By contrast, photoreceptors overexpressing Amph have an abnormal punctate 'ball' of F-actin and Bifocal at the apical cortex (Fig. 6D,F) and Amph is delocalized from the apical membrane (Fig. 6G,H). We conclude that excess Amph protein leads to destabilization of the normal apical Amph localization, a mislocalization of Bifocal protein and F-actin, and the subsequent failure in rhabdomere morphogenesis.

These data lead to the following model for Amph function. Bifocal is localized to the apical membrane of photoreceptor neurons, where it recruits Amph and other proteins. This protein complex then aids in the morphogenesis of the intricately folded rhabdomere membrane. Loss of Amph results in a mild phenotype, perhaps because Bifocal and additional proteins are still apically localized and can promote rhabdomere morphogenesis. However, when Amph is mislocalized outside of the apical membrane domain (in Amph overexpression experiments or in *bifocal* mutants), it can induce the formation of ectopic rhabdomere membrane domains or inhibit rhabdomere morphogenesis by relocating or titrating away the necessary protein complex to form a rhabdomere.

DISCUSSION

Drosophila Amphiphysin is an ortholog of Amph II

All known Amph family proteins contain a N-terminal coiled-coil domain and a C-terminal SH3 domain with a variable central domain. In Amph I and Amph II, the central domain provides an additional link to endocytosis via the inclusion of binding sites for clathrin and α-Adaptin (Slepnev et al., 2000). Although sequence comparison does not clearly indicate whether *Drosophila* Amph is more related to either vertebrate Amph I or Amph II, examination of expression profiles, isoform organization and inferred functions suggest that *Drosophila* Amph is likely to be an Amph II ortholog.

First, both *Drosophila* Amph and vertebrate Amph II have a broad tissue distribution, including postsynaptic expression in skeletal muscle (Butler et al., 1997). Second, both *Drosophila* Amph and Amph II genes have isoforms that partially or completely remove the central domain (Fig. 1B) (Butler et al., 1997). Third, we show that *Drosophila* Amph is sufficient to organize membrane morphogenesis in photoreceptor neurons and necessary for protein localization at the postsynaptic NMJ. Similarly, the putative localization of Amph II to nodes of Ranvier and the localization of yeast Rvs167 to the protruding bud and schmoo membranes, suggests that Amph II and Rvs167 may be involved in regulating membrane morphogenesis, rather than endocytosis.

The absence of detectable endocytic defects in synaptic vesicle recycling in *amph* mutants is surprising, given the evidence linking Amph and synaptic vesicle endocytosis in vertebrate systems (Wigge and McMahon, 1998). Our results cannot completely eliminate a role of Amph in endocytosis. We find Amph protein on vesicles within cells known to be actively undergoing endo- and exocytosis, such as the hindgut, garland gland and salivary gland. A detailed characterization of the *amph* phenotype in these cells may ultimately reveal a role for Amph in regulating endocytosis.

Membrane morphogenesis and protein localization

There are two common features of Amph expression. First, Amph always localizes to a restricted subcellular membrane domain, typically the apical membrane in epithelial or neuronal cells. Second, Amph is detected at membranes that are undergoing 'remodeling' or morphogenesis. During cellularization, the addition of membrane occurs at defined sites and in a precise sequence (Lecuit and Wieschaus, 2000). Amph localization precisely correlates with the bi-phasic insertion of new membrane: first apical and then apical-lateral. In the tubular tracheal system, Amph is localized to the inner (apical) membrane domain. It has been hypothesized that tracheal tube size is controlled by regulating surface area of the apical membrane: during tracheal tube dilation, the inner (apical) diameter of the tube increases dramatically, whereas the outer (basal) diameter shows little or no change (Beitel and Krasnow, 2000). Thus, Amph is present on the membrane domain that undergoes regulated alteration in curvature and surface area and as such might regulate the changes observed. Similarly, the Amph-related yeast Rvs167 protein is localized to the protruding bud or schmoo membrane (Balguerie et al., 1999), another actively 'remodeled' membrane domain.

Not only do we see Amph detected at membranes undergoing elongation or changes in surface area, we also detect Amph at highly folded membrane domains. For example, each photoreceptor rhabdomere is an interconnected stack of membranes that emerges from the apical neuronal membrane. The process of rhabdomere site selection, initiation, and elaboration is poorly understood. Our results indicate a role for Amph in organizing the intricately folded rhabdomere membrane. First, accumulation of Amph on the apical surface occurs together with an enrichment of F-actin at this site. Second, overexpression of Amph (by targeted misexpression or in *bifocal* mutants) results in the delocalization of endogenous Amph and the mislocalization of both F-actin, leading to either loss or ectopic rhabdomeres. Loss of rhabdomeres may be due to excess Amph titrating out

factors necessary for the proper development of rhabdomeres; ectopic rhabdomeres may be due to ectopic Amph recruiting sufficient F-actin or other proteins to a second site in the cell and thus triggering formation of an extra rhabdomere.

The development or maintenance of a cellular three-dimensional structure, like a rhabdomere or synapse, not only includes the rearrangement of the membrane and actin cytoskeleton but also involves the correct targeting and anchoring of proteins to these locations. Consistent with a role in protein targeting/anchoring, we find that in *amph* null mutants multiple postsynaptic proteins are mislocalized. Dlg and Scrib are partially delocalized, and Lgl is completely undetectable at the postsynaptic membrane (although Lgl staining at the muscle M line is unaffected). These defects are not due to a general delocalization of all postsynaptic proteins, as we observe normal localization of two different epitope-tagged glutamate receptors to the postsynaptic membrane.

How does the removal of Amph result in the delocalization of Lgl, Dlg and Scrib at the synapse? One possibility is that Amph may play a role in the establishment or maintenance of postsynaptic membrane structure. One characteristic of type I synapses is that they have an extensive subsynaptic reticulum, the highly folded membrane surrounding the synapse, that is not present in type II and type III synapses. *amph* mutants may have defects in the folded membrane that do not allow for proper retention of proteins at the synapse. Alternatively, Amph may act as a localized scaffold protein that recruits Lgl to the postsynaptic membrane, with Lgl being necessary for proper anchoring or targeting of Dlg and Scrib. This would be consistent with the known role of Lgl in mediating Dlg and Scrib localization in epithelia (Bilder et al., 2000). Lgl belongs to a family of proteins that regulate polarized exocytosis and protein targeting to specific membrane domains (Fujita et al., 1998; Lehman et al., 1999; Ohshiro et al., 2000; Peng et al., 2000). In addition, deletion analysis of Dlg has identified a two-step process of synaptic targeting: Dlg is first targeted to the muscle plasma membrane and then to the subsynaptic reticulum (Thomas et al., 2000). Loss of Amph function gives a phenotype consistent with a failure in the second step of this process; however, we have been unable to detect direct interactions between Amph and Dlg proteins in vitro (data not shown). Further analysis of the physical interactions between Amph and Lgl, Dlg or Scrib may help illuminate the mechanism of postsynaptic protein localization, and the analysis of *lgl* and *scrib* synaptic phenotypes will be required to determine whether the functional defects at *amph* mutant synapses (increase in quantal size) are due to the mislocalization of Lgl, Dlg or Scrib.

Does Amphiphysin link the actin cytoskeleton with membrane morphogenesis?

How does Amph regulate membrane morphogenesis? Amph could directly regulate the actin cytoskeleton, leading to changes in membrane topology. Alternatively, Amph could directly modify membrane structure, and only indirectly affect the actin cytoskeleton. These models are not mutually exclusive. The latter model (direct membrane bending) is supported by studies of mammalian Amph I, which show that Amph can directly bind lipid bilayers and distort them into high-curvature membranes; for example, Amph I can transform spherical liposomes into narrow tubules (Takei et al., 1999). The former model (actin regulation) is supported by work on yeast, *Drosophila* and vertebrate Amph proteins. First, there is the tight correlation between Amph expression and actin organization in all organisms tested: yeast bud and schmoo membrane extensions, and *Drosophila* cellularization and rhabdomere formation; and vertebrate nodes of Ranvier are all sites of F-actin enrichment and Amph localization. Second, our results show that the delocalization of Amph from the apical surface of photoreceptor cells, in *bifocal* mutants or *amph* overexpression mutants, results in the mislocalization of F-actin. Last, in yeast, this idea is supported by the identification of a protein interaction between Rvs167 SH3 domain and actin binding protein Abp1 (Lila and Drubin, 1997) as well as synthetic lethality between *rvs167* and a subset of actin *act1* alleles (Breton and Aigle, 1998). In *Drosophila*, it is currently unknown what protein(s) bind to the Amph SH3 domain; it will be interesting to determine if a similar actin-binding protein-SH3 domain interaction occurs in *Drosophila*. This type of biochemical analysis, as well as further genetic studies, will be necessary to understand the relationship between Amph, the actin cytoskeleton and membrane morphogenesis.

We thank Drs W. Chia, C. Goodman, M. Krasnow, M. Ramaswami, P. Bryant and the Developmental Studies Hybridoma Bank for reagents. In addition, we acknowledge the free exchange of reagents with Dr C. O'Kane and his support of Dr A. Razzaq. We also thank Drs Y. Goda, M. Freeman, K. Siller and T. Avidor-Reiss for their comments on the manuscript. A. C. Z expresses gratitude to Drs William McGinnis and Charles Zuker for providing space and supplies for the completion of this study. A. C. Z was supported by a Damon Runyon-Walter Winchell Foundation Fellowship (DRG-1478) and by a NIH NSRA (DC00432-02). Work in the laboratory of B. Z. is supported by the University of Texas and by an NSF Career Award (IBN-0093170). C. Q. D is an Associate Investigator of the HHMI.

REFERENCES

Anderson, M. S., Halpern, M. E. and Keshishian, H. (1988). Identification of the neuropeptide transmitter proctolin in Drosophila larvae: characterization of muscle fiber-specific neuromuscular endings. *J. Neurosci.* **8**, 242-255.

Atwood, H. L., Govind, C. K. and Wu, C. F. (1993). Differential ultrastructure of synaptic terminals on ventral longitudinal abdominal muscles in Drosophila larvae. *J. Neurobiol.* **24**, 1008-1024.

Bahri, S. M., Yang, X. and Chia, W. (1997). The Drosophila bifocal gene encodes a novel protein which colocalizes with actin and is necessary for photoreceptor morphogenesis. *Mol. Cell. Biol.* **17**, 5521-5529.

Baker, E. K., Colley, N. J. and Zuker, C. S. (1994). The cyclophilin homolog NinaA functions as a chaperone, forming a stable complex in vivo with its protein target rhodopsin. *EMBO J.* **13**, 4886-4895.

Balguerie, A., Sivadon, P., Bonneu, M. and Aigle, M. (1999). Rvs167p, the budding yeast homolog of amphiphysin, colocalizes with actin patches. *J. Cell Sci.* **112**, 2529-2537.

Bauer, F., Urdaci, M., Aigle, M. and Crouzet, M. (1993). Alteration of a yeast SH3 protein leads to conditional viability with defects in cytoskeletal and budding patterns. *Mol. Cell. Biol.* **13**, 5070-5084.

Beitel, G. J. and Krasnow, M. A. (2000). Genetic control of epithelial tube size in the Drosophila tracheal system. *Development* **127**, 3271-3282.

Bilder, D., Li, M. and Perrimon, N. (2000). Cooperative regulation of cell polarity and growth by Drosophila tumor suppressors. *Science* **289**, 113-116.

Brand, A. H. and Perrimon, N. (1993). Targeted gene expression as a means of altering cell fates and generating dominant phenotypes. *Development* **118**, 401-415.

Breton, A. M. and Aigle, M. (1998). Genetic and functional relationship between Rvsp, myosin and actin in Saccharomyces cerevisiae. *Curr. Genet.* **34**, 280-286.

Budnik, V., Zhong, Y. and Wu, C. F. (1990). Morphological plasticity of motor axons in Drosophila mutants with altered excitability. *J. Neurosci.* **10**, 3754-3768.

Butler, M. H., David, C., Ochoa, G. C., Freyberg, Z., Daniell, L., Grabs, D., Cremona, O. and De Camilli, P. (1997). Amphiphysin II (SH3P9; BIN1), a member of the amphiphysin/Rvs family, is concentrated in the cortical cytomatrix of axon initial segments and nodes of ranvier in brain and around T tubules in skeletal muscle. *J. Cell Biol.* **137**, 1355-1367.

Cantera, R. and Nassel, D. R. (1992). Segmental peptidergic innervation of abdominal targets in larval and adult dipteran insects revealed with an antiserum against leucokinin I. *Cell Tissue Res.* **269**, 459-471.

David, C., McPherson, P. S., Mundigl, O. and de Camilli, P. (1996). A role of amphiphysin in synaptic vesicle endocytosis suggested by its binding to dynamin in nerve terminals. *Proc. Natl. Acad. Sci. USA* **93**, 331-335.

DiAntonio, A., Petersen, S. A., Heckmann, M. and Goodman, C. S. (1999). Glutamate receptor expression regulates quantal size and quantal content at the Drosophila neuromuscular junction. *J. Neurosci.* **19**, 3023-3032.

Fujita, Y., Shirataki, H., Sakisaka, T., Asakura, T., Ohya, T., Kotani, H., Yokoyama, S., Nishioka, H., Matsuura, Y., Mizoguchi, A. et al. (1998). Tomosyn: a syntaxin-1-binding protein that forms a novel complex in the neurotransmitter release process. *Neuron* **20**, 905-915.

Gonzalez-Gaitan, M. and Jackle, H. (1997). Role of Drosophila alpha-adaptin in presynaptic vesicle recycling. *Cell* **88**, 767-776.

Gorczyca, M., Augart, C. and Budnik, V. (1993). Insulin-like receptor and insulin-like peptide are localized at neuromuscular junctions in Drosophila. *J. Neurosci.* **13**, 3692-3704.

Grabs, D., Slepnev, V. I., Songyang, Z., David, C., Lynch, M., Cantley, L. C. and De Camilli, P. (1997). The SH3 domain of amphiphysin binds the proline-rich domain of dynamin at a single site that defines a new SH3 binding consensus sequence. *J. Biol. Chem.* **272**, 13419-13425.

Jia, X. X., Gorczyca, M. and Budnik, V. (1993). Ultrastructure of neuromuscular junctions in Drosophila: comparison of wild type and mutants with increased excitability. *J. Neurobiol.* **24**, 1025-1044.

Lahey, T., Gorczyca, M., Jia, X. X. and Budnik, V. (1994). The Drosophila tumor suppressor gene dlg is required for normal synaptic bouton structure. *Neuron* **13**, 823-835.

Lecuit, T. and Wieschaus, E. (2000). Polarized insertion of new membrane from a cytoplasmic reservoir during cleavage of the Drosophila embryo. *J. Cell Biol.* **150**, 849-860.

Lehman, K., Rossi, G., Adamo, J. E. and Brennwald, P. (1999). Yeast homologues of tomosyn and lethal giant larvae function in exocytosis and are associated with the plasma membrane SNARE, Sec9. *J. Cell Biol.* **146**, 125-140.

Lichte, B., Veh, R. W., Meyer, H. E. and Kilimann, M. W. (1992). Amphiphysin, a novel protein associated with synaptic vesicles. *EMBO J.* **11**, 2521-2530.

Lila, T. and Drubin, D. G. (1997). Evidence for physical and functional interactions among two Saccharomyces cerevisiae SH3 domain proteins, an adenylyl cyclase-associated protein and the actin cytoskeleton. *Mol. Biol. Cell* **8**, 367-385.

Lloyd, T. E., Verstreken, P., Ostrin, E. J., Phillippi, A., Lichtarge, O. and Bellen, H. J. (2000). A genome-wide search for synaptic vesicle cycle proteins in Drosophila. *Neuron* **26**, 45-50.

McDonald, J. A. and Doe, C. Q. (1997). Establishing neuroblast-specific gene expression in the Drosophila CNS: huckebein is activated by Wingless and Hedgehog and repressed by Engrailed and Gooseberry. *Development* **124**, 1079-1087.

McPherson, P. S., Garcia, E. P., Slepnev, V. I., David, C., Zhang, X., Grabs, D., Sossin, W. S., Bauerfeind, R., Nemoto, Y. and De Camilli, P. (1996). A presynaptic inositol-5-phosphatase. *Nature* **379**, 353-357.

Monastirioti, M., Gorczyca, M., Rapus, J., Eckert, M., White, K. and Budnik, V. (1995). Octopamine immunoreactivity in the fruit fly Drosophila melanogaster. *J. Comp. Neurol.* **356**, 275-287.

Ohshiro, T., Yagami, T., Zhang, C. and Matsuzaki, F. (2000). Role of cortical tumour-suppressor proteins in asymmetric division of Drosophila neuroblast. *Nature* **408**, 593-596.

Peng, C. Y., Manning, L., Albertson, R. and Doe, C. Q. (2000). The tumour-suppressor genes lgl and dlg regulate basal protein targeting in Drosophila neuroblasts. *Nature* **408**, 596-600.

Ramjaun, A. R., Micheva, K. D., Bouchelet, I. and McPherson, P. S. (1997). Identification and characterization of a nerve terminal-enriched amphiphysin isoform. *J. Biol. Chem.* **272**, 16700-16706.

Razzaq, A., Su, Y., Mehren, J. E., Mizuguchi, K., Jackson, A. P., Gay, N. J. and O'Kane, C. J. (2000). Characterisation of the gene for Drosophila amphiphysin. *Gene* **241**, 167-174.

Rorth, P. (1996). A modular misexpression screen in Drosophila detecting tissue-specific phenotypes. *Proc. Natl. Acad. Sci. USA* **93**, 12418-12422.

Rorth, P., Szabo, K., Bailey, A., Laverty, T., Rehm, J., Rubin, G. M., Weigmann, K., Milan, M., Benes, V., Ansorge, W. et al. (1998). Systematic gain-of-function genetics in Drosophila. *Development* **125**, 1049-1057.

Shupliakov, O., Low, P., Grabs, D., Gad, H., Chen, H., David, C., Takei, K., De Camilli, P. and Brodin, L. (1997). Synaptic vesicle endocytosis impaired by disruption of dynamin-SH3 domain interactions. *Science* **276**, 259-263.

Sivadon, P., Bauer, F., Aigle, M. and Crouzet, M. (1995). Actin cytoskeleton and budding pattern are altered in the yeast rvs161 mutant: the Rvs161 protein shares common domains with the brain protein amphiphysin. *Mol. Gen. Genet.* **246**, 485-495.

Sivadon, P., Crouzet, M. and Aigle, M. (1997). Functional assessment of the yeast Rvs161 and Rvs167 protein domains. *FEBS Lett.* **417**, 21-27.

Slepnev, V. I., Ochoa, G. C., Butler, M. H. and De Camilli, P. (2000). Tandem arrangement of the clathrin and AP-2 binding domains in amphiphysin 1 and disruption of clathrin coat function by amphiphysin fragments comprising these sites. *J. Biol. Chem.* **275**, 17583-17589.

Takei, K., Slepnev, V. I., Haucke, V. and De Camilli, P. (1999). Functional partnership between amphiphysin and dynamin in clathrin-mediated endocytosis. *Nat. Cell Biol.* **1**, 33-39.

Thomas, U., Ebitsch, S., Gorczyca, M., Koh, Y. H., Hough, C. D., Woods, D., Gundelfinger, E. D. and Budnik, V. (2000). Synaptic targeting and localization of discs-large is a stepwise process controlled by different domains of the protein. *Curr. Biol.* **10**, 1108-1117.

Umbach, J. A., Zinsmaier, K. E., Eberle, K. K., Buchner, E., Benzer, S. and Gundersen, C. B. (1994). Presynaptic dysfunction in Drosophila csp mutants. *Neuron* **13**, 899-907.

Wigge, P. and McMahon, H. T. (1998). The amphiphysin family of proteins and their role in endocytosis at the synapse. *Trends Neurosci.* **21**, 339-344.

Wigge, P., Vallis, Y. and McMahon, H. T. (1997). Inhibition of receptor-mediated endocytosis by the amphiphysin SH3 domain. *Curr. Biol.* **7**, 554-560.

Zelhof, A. C., Ghbeish, N., Tsai, C., Evans, R. M. and McKeown, M. (1997). A role for ultraspiracle, the Drosophila RXR, in morphogenetic furrow movement and photoreceptor cluster formation. *Development* **124**, 2499-2506.

Zhang, B., Koh, Y. H., Beckstead, R. B., Budnik, V., Ganetzky, B. and Bellen, H. J. (1998). Synaptic vesicle size and number are regulated by a clathrin adaptor protein required for endocytosis. *Neuron* **21**, 1465-1475.

Zinsmaier, K. E., Eberle, K. K., Buchner, E., Walter, N. and Benzer, S. (1994). Paralysis and early death in cysteine string protein mutants of Drosophila. *Science* **263**, 977-980.